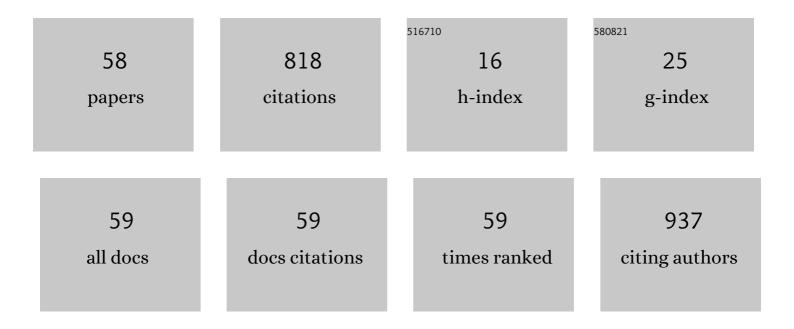
## Hiroyuki Muto

List of Publications by Year in descending order

Source: https://exaly.com/author-pdf/8529479/publications.pdf Version: 2024-02-01



#	Article	IF	CITATIONS
1	Mechanical properties of alumina matrix composite reinforced with carbon nanofibers affected by small interfacial sliding shear stress. Ceramics International, 2022, 48, 8466-8472.	4.8	7
2	Transparent conductive polymer composites obtained via electrostatically assembled carbon nanotubes–poly (methyl methacrylate) composite particles. Advanced Powder Technology, 2022, 33, 103528.	4.1	8
3	Ionic Conduction and Electric Modulus in Li <sub>2</sub> S–CaS and Ca <i>X</i> <sub>2</sub> ( <i>X</i> = F, Cl, Br, and I) Nanocomposites. Electrochemistry, 2022, 90, 067005-067005.	1.4	4
4	Ordered arrays of electrostatically assembled SiO2–SiO2 composite particles by electrophoresis-induced stimulation. Journal of Sol-Gel Science and Technology, 2022, 104, 548-557.	2.4	1
5	Controlled formation of carbon nanotubes incorporated ceramic composite granules by electrostatic integrated nano-assembly. Nanoscale, 2022, 14, 9669-9674.	5.6	4
6	Current progress in the development of Fe-air batteries and their prospects for next-generation batteries. , 2021, , 59-83.		5
7	Nanomaterial Fabrication through the Modification of Sol–Gel Derived Coatings. Nanomaterials, 2021, 11, 181.	4.1	36
8	Electrostatically assembled SiC–Al2O3 composite particles for direct selective laser sintering. Advanced Powder Technology, 2021, 32, 2074-2084.	4.1	8
9	Development of liquid-phase fabrication of nanotube array-based multiferroic nanocomposite film. Journal of Alloys and Compounds, 2021, 869, 159219.	5.5	2
10	Nanoporous anodic Nb2O5 with pore-in-pore structure formation and its application for the photoreduction of Cr(VI). Chemosphere, 2021, 283, 131231.	8.2	13
11	Preparation of catalytically active Au nanoparticles by sputter deposition and their encapsulation in metal-organic framework of Cu3(BTC)2. Materials Letters, 2020, 261, 127124.	2.6	8
12	Incorporation of titanium pyrophosphate in polybenzimidazole membrane for medium temperature dry PEFC application. Solid State Ionics, 2020, 344, 115140.	2.7	16
13	Fe3O4-embedded rGO composites as anode for rechargeable FeOx-air batteries. Materials Today Communications, 2020, 25, 101540.	1.9	18
14	Formation of Feâ€embedded graphitic carbon network composites as anode materials for rechargeable Feâ€eir batteries. Energy Storage, 2020, 2, e196.	4.3	4
15	Electrostatic Assembly Technique for Novel Composites Fabrication. Journal of Composites Science, 2020, 4, 155.	3.0	15
16	Catalytically active PdRu and CuRu bimetallic nanoparticle formation in the mesoporous SiO2 by supercritical CO2-assisted immobilization. Journal of Supercritical Fluids, 2020, 160, 104818.	3.2	1
17	Improved green body strength using PMMA–Al <sub>2</sub> O <sub>3</sub> composite particles fabricated via electrostatic assembly. Nano Express, 2020, 1, 030001.	2.4	4
18	Formation of porous Al <sub>2</sub> 0 <sub>3</sub> –SiO <sub>2</sub> composite ceramics by electrostatic assembly. Journal of the Ceramic Society of Japan, 2020, 128, 605-610.	1.1	7

Нігочикі Мито

#	Article	IF	CITATIONS
19	Design of Heat-Conductive hBN–PMMA Composites by Electrostatic Nano-Assembly. Nanomaterials, 2020, 10, 134.	4.1	12
20	Antibacterial and antifungal properties of Ag nanoparticle-loaded cellulose nanofiber aerogels prepared by supercritical CO2 drying. Journal of Supercritical Fluids, 2019, 143, 1-7.	3.2	39
21	Nanotube array-based barium titanate–cobalt ferrite composite film for affordable magnetoelectric multiferroics. Journal of Materials Chemistry C, 2019, 7, 10066-10072.	5.5	19
22	Effect of mixed alkali metal ions in highly proton conductive K/Cs-hydrogen sulfate-phosphotungstic acid composites prepared by mechanical milling. Solid State Ionics, 2019, 340, 115022.	2.7	4
23	Controlled microstructure and mechanical properties of Al2O3-based nanocarbon composites fabricated by electrostatic assembly method. Nanoscale Research Letters, 2019, 14, 245.	5.7	12
24	PMMA-ITO Composite Formation via Electrostatic Assembly Method for Infra-Red Filtering. Nanomaterials, 2019, 9, 886.	4.1	20
25	Facile formation of Fe3O4-particles decorated carbon paper and its application for all-solid-state rechargeable Fe-air battery. Applied Surface Science, 2019, 486, 257-264.	6.1	17
26	Fabrication of an all-solid-state Zn-air battery using electroplated Zn on carbon paper and KOH-ZrO2 solid electrolyte. Applied Surface Science, 2019, 487, 343-348.	6.1	21
27	Anhydrous proton conductive xCHS-(1-x)WSiA composites prepared via liquid-phase shaking. Solid State Ionics, 2019, 337, 1-6.	2.7	3
28	Investigation of the anchor layer formation on different substrates and its feasibility for optical properties control by aerosol deposition. Applied Surface Science, 2019, 483, 212-218.	6.1	13
29	Effects of cesium-substituted silicotungstic acid doped with polybenzimidazole membrane for the application of medium temperature polymer electrolyte fuel cells. E3S Web of Conferences, 2019, 83, 01008.	0.5	4
30	Fabrication of Carbon-decorated Al <sub>2</sub> O <sub>3</sub> Composite Powders using Cellulose Nanofiber for Selective Laser Sintering. Funtai Oyobi Fummatsu Yakin/Journal of the Japan Society of Powder and Powder Metallurgy, 2019, 66, 168-173.	0.2	7
31	Micro- and Nano-assembly of Composite Particles by Electrostatic Adsorption. Nanoscale Research Letters, 2019, 14, 297.	5.7	25
32	Electrical and Thermal Properties of PMMA/h-BN Composite Material Produced by Electrostatic Adsorption Method. IEEJ Transactions on Fundamentals and Materials, 2019, 139, 60-65.	0.2	4
33	Preparation of LiNi <sub>1/3</sub> Mn <sub>1/3</sub> Co <sub>1/3</sub> O <sub>2cathode composite particles using a new liquid-phase process and application to all-solid-state lithium batteries. Journal of the Ceramic Society of Japan. 2018. 126. 826-831.</sub>	ıb>/Li&l	t;suþ>3⁢
34	Cell performance enhancement with titania-doped polybenzimidazole based composite membrane in intermediate temperature fuel cell under anhydrous condition. Journal of the Ceramic Society of Japan, 2018, 126, 789-793.	1.1	11
35	Sol-gel template synthesis of BaTiO3 films with nano-periodic structures. Materials Letters, 2018, 227, 120-123.	2.6	7
36	Multiferroic nanocomposite fabrication via liquid phase using anodic alumina template. Science and Technology of Advanced Materials, 2018, 19, 535-542.	6.1	5

Нігочикі Мито

#	Article	IF	CITATIONS
37	Nano/Microcomposite Particles: Preparation Processes and Applications. , 2018, , 781-785.		1
38	Ag nanoparticle-filled TiO <sub>2</sub> nanotube arrays prepared by anodization and electrophoretic deposition for dye-sensitized solar cells. Nanotechnology, 2017, 28, 135207.	2.6	25
39	Development of Iron-Based Rechargeable Batteries with Sintered Porous Iron Electrodes. ECS Transactions, 2017, 75, 111-116.	O.5	5
40	Supercritical fluid-assisted immobilization of Pd nanoparticles in the mesopores of hierarchical porous SiO2 for catalytic applications. Journal of Supercritical Fluids, 2017, 130, 140-146.	3.2	21
41	Electrochemical Performance of Sintered Porous Negative Electrodes Fabricated with Atomized Powders for Iron-Based Alkaline Rechargeable Batteries. Journal of the Electrochemical Society, 2017, 164, A2049-A2055.	2.9	14
42	Influence of Orientation of Flaky Boron Nitride on Electrical and Thermal Properties of Polymethylmethacrylate / Boron Nitride Electrical Insulating Composite Material Produced by Electrostatic Adsorption Method. IEEJ Transactions on Fundamentals and Materials, 2017, 137, 202-207.	0.2	1
43	Chemical synthesis of Li3PS4 precursor suspension by liquid-phase shaking. Solid State Ionics, 2016, 285, 2-5.	2.7	69
44	Catalytically active Pt nanoparticles immobilized inside the pores of metal organic framework using supercritical CO2 solutions. Microporous and Mesoporous Materials, 2016, 225, 26-32.	4.4	39
45	Production of Thermal Conductive PMMA/BN Electric Insulating Composite Material using Electrostatic Adsorption Method. IEEJ Transactions on Fundamentals and Materials, 2016, 136, 186-192.	0.2	2
46	Ag nanoparticle-deposited TiO2 nanotube arrays for electrodes of Dye-sensitized solar cells. Nanoscale Research Letters, 2015, 10, 219.	5.7	33
47	Blue-emitting photoluminescence of rod-like and needle-like ZnO nanostructures formed by hot-water treatment of sol–gel derived coatings. Journal of Luminescence, 2015, 158, 44-49.	3.1	14
48	Preparation of Exoergic Insulating Composite Material using Electrostatic Adsorption Method. IEEJ Transactions on Fundamentals and Materials, 2015, 135, 217-222.	0.2	4
49	Preparation of hydroxide ion conductive KOH-ZrO2 electrolyte for all-solid state iron/air secondary battery. Solid State Ionics, 2014, 262, 188-191.	2.7	9
50	<b>Preparation of hydroxide ion conductive KOH–layered double hydroxide electrolytes for an all-solid-state iron–air secondary battery</b> . Journal of Asian Ceramic Societies, 2014, 2, 165-168.	2.3	16
51	Enhanced dye-sensitized solar cells performance of ZnO nanorod arrays grown by low-temperature hydrothermal reaction. International Journal of Energy Research, 2013, 37, n/a-n/a.	4.5	12
52	Characterization of mechanochemically synthesized MHSO4–H4SiW12O40 composites (M=K, NH4, Cs). Materials Research Bulletin, 2012, 47, 2931-2935.	5.2	6
53	Anhydrous proton conductivity of KHSO4–H3PW12O40 composites and the correlation with hydrogen bonding distance under ambient pressure. Electrochimica Acta, 2011, 56, 9364-9369.	5.2	18
54	Solid-state mechanochemical synthesis of CsHSO4 and 1,2,4-triazole inorganic–organic composite electrolytes for dry fuel cells. Electrochimica Acta, 2011, 56, 2364-2371.	5.2	12

Нігочикі Мито

#	Article	IF	CITATIONS
55	Mechanochemically synthesized CsH <sub>2</sub> PO <sub>4</sub> –H <sub>3</sub> PW <sub>12</sub> O <sub>40</sub> composites as proton-conducting electrolytes for fuel cell systems in a dry atmosphere. Science and Technology of Advanced Materials, 2011, 12, 034402.	6.1	14
56	Inorganic–organic composite electrolytes consisting of polybenzimidazole and Cs-substituted heteropoly acids and their application for medium temperature fuel cells. Journal of Materials Chemistry, 2010, 20, 6359.	6.7	77
57	Three-dimensional hydrogen-bonding networks and proton conductivities under non-humidified conditions of CsHSO4–WPA composites. Solid State Ionics, 2010, 181, 180-182.	2.7	15
58	Mechanochemically synthesized cesium-ion-substituted phosphotungstic acid using several types of cesium-containing salts. Solid State Ionics, 2008, 179, 1174-1177.	2.7	19